

Millimeter-wave High-Efficiency Multilayer Parasitic Microstrip Antenna Array for System-on-package

Tomohiro Seki, Kenjiro Nishikawa[†], Ichihiko Toyoda, and Koichi Tsunekawa

Abstract

This paper describes the design and characteristics of a highly efficient multilayer parasitic microstrip antenna array (MPMAA) constructed on a multilayer substrate for millimeter-wave system-on-package modules. The antenna on a Teflon substrate achieved a radiation efficiency of greater than 91% and an associated antenna gain of 11.1 dBi at 60 GHz. Its size is only 10 mm × 10 mm. We discuss MPMAAs fabricated on both Teflon and low-temperature cofired ceramic (LTCC) substrates. The measured performances of prototype antennas are also presented. The MPMAA offers compactness and high efficiency and is easily integrated with the system-on-package design. It will lead to compact and cost-effective millimeter-wave RF modules.

1. Introduction

The strong demand for high-speed wireless applications has stimulated the development of millimeter-wave and quasi-millimeter-wave wireless equipment [1]-[3]. V-band (50–75 GHz) wireless systems are very interesting because they offer much higher transmission rates, above 1 Gbit/s, due to their wider bandwidths. These applications require compact, high-performance, and cost-effective wireless equipment. A highly integrated RF (radio frequency) module, known as a system-on-package module, which has a multilayer structure, is effective in meeting these requirements [4]-[7]. It is necessary to use active integrated antenna technology to make a module integrated with antennas that consume little power and have low-noise characteristics [8]-[10].

Several approaches to achieve an RF module integrated with antennas have been reported.

1) One approach is a semiconductor on-chip antenna such as a microstrip antenna (MSA) that is integrated with RF circuits on the same semiconductor substrate [4]. However, in this approach it is difficult

to establish a high-gain antenna having an antenna array configuration on a semiconductor substrate due to the substrate's size and loss. Therefore, high-gain compact antennas have not yet been integrated with monolithic microwave integrated circuits (MMICs).

2) A multi-chip module approach has also been proposed for a module integrated with antennas [5], [6]. In this module, antennas and MMICs are connected by wire bonding or a ribbon, which results in a high connection loss. This approach also requires a low-loss feeding circuit.

3) A dielectric lens antenna has been used to achieve a high-gain antenna [7]. However, the commonly used lens antenna is constructed using an expensive crystal material and it is difficult to mount it on the MMIC package. Thus, a dielectric lens antenna fabricated using resin was investigated as a low cost alternative.

There are problems, however, in mounting the antenna on the MMIC package and achieving high efficiency. Moreover, it is difficult to construct an antenna array substrate on a single layer due to the limitations of the manufacturing process for the millimeter-wave frequency band.

A technique for improving the radiation efficiency by arranging parasitic elements above the feeding microstrip antenna elements has been investigated

[†] NTT Network Innovation Laboratories
Yokosuka-shi, 239-0847 Japan
E-mail: nisikawa.kenjiro@lab.ntt.co.jp

[11]-[15]. However, obtaining a sufficient absolute gain was difficult in these studies [11]-[14]. A high gain antenna using a low-permittivity layer or an air layer has been investigated, but only the directional gain was described and it was difficult to use this antenna in a system-on-package design due to the parasitic element substrates.

To overcome the above problems, we are studying a multilayer parasitic microstrip antenna array (MPMAA) structure based on a parasitic antenna configuration [16], [17]. This paper describes a highly efficient MPMAA structure for a system-on-package module at millimeter-wave frequency bands. At 60 GHz, the antenna on a Teflon substrate achieves high radiation efficiency of greater than 91% and high gain of greater than 11.1 dBi. The rest of this paper is organized as follows. Section 2 describe the concept of the system-on-package module and the design of the antenna. Section 3 presents the effect of the alignment precision of the manufacturing process. Finally, Section 4 presents measurement results for prototype 60-GHz band antennas fabricated on Teflon and low-temperature cofired ceramic (LTCC)* substrates. Our MPMAA offers compactness and high-efficiency performance for millimeter-wave system-on-package modules.

2. Design of parasitic element arrangement on Teflon substrate

2.1 Concept of millimeter-wave system-on-package

The concept of a system-on-package module integrated with an antenna is shown in Fig. 1. An MPMAA and a highly integrated transceiver MMIC are mounted on a multilayer structure, in a vertical stacking configuration. Two types of feeding methods for the MPMAA are considered. In the first method, a feeding element is constructed on the MMIC chip, and the MPMAA is fed by electromagnetic coupling without a feeding line. In the other, a feeding element is constructed where the multilayer substrate of the MPMAA and the element are connected to the terminal of the MMIC using flip-chip technology. As indicated in Fig. 1, the MPMAA uses two parasitic layers with four parasitic elements on each layer.

2.2 MPMAA design

This antenna achieves high gain because it increases the antenna aperture by utilizing the coupling

between the layers of the multilayer substrate. Here, we describe the MPMAA design for the 60-GHz band. We use the moment method as the calculation method and assume that the ground plane is infinite. To clarify the MPMAA's characteristics, we use a multilayer Teflon substrate ($\epsilon_r = 2.2$, $\tan\delta = 0.0007$ at 10 GHz) as the antenna substrate. The MPMAA on the Teflon substrate also exhibits excellent characteristics such as a high gain and a wide bandwidth. A simulation model for the MPMAA is shown in Fig. 2. Here, we use the via-fed method for the feeding method. The size of the feeding element is $0.30 \lambda_0 \times 0.30 \lambda_0$ and the feeding point is $0.01 \lambda_0$ away from the center of the patch, where λ_0 is the free-space wavelength. The size of the parasitic elements mounted on the first parasitic layer is $0.32 \lambda_0 \times 0.32 \lambda_0$ and the patch size of the second parasitic layer is $0.28 \lambda_0 \times 0.28 \lambda_0$. The four parasitic elements mounted on the

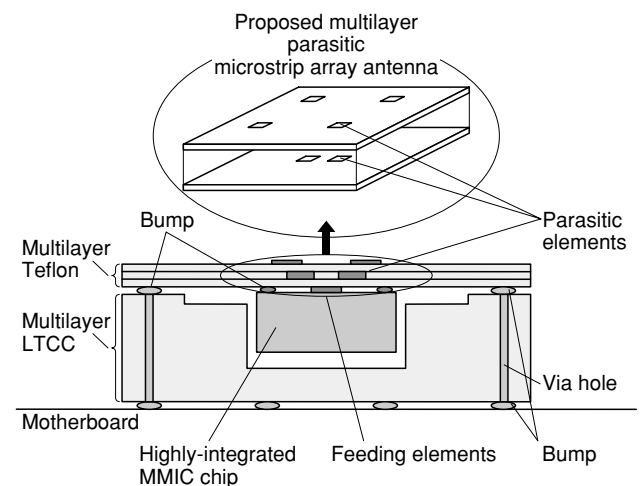


Fig. 1. Novel structure of system-on-package integrated with antenna.

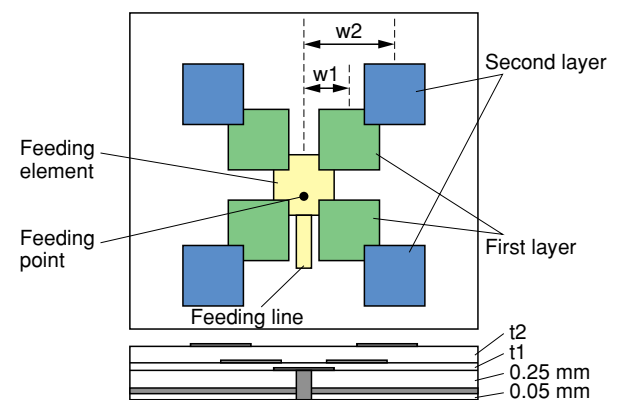


Fig. 2. Antenna model.

* LTCC is a glass ceramics to be fired at around 900°C.

first parasitic layer are arranged so that they are equidistant from the center of the feeding MSA. For convenience, the width (horizontal direction) is expressed so that the widths of the first and second parasitic layers are w_1 and w_2 , respectively. In addition, t_1 and t_2 represent the substrate thicknesses of the first and second parasitic layers, respectively. The relationship between w_1 and w_2 that yields the maximum absolute gain is shown in **Fig. 3**. Here, t_1 and t_2 were set to 0.25 and 0.55 mm, respectively. In this figure, it is clear that w_1 is proportional to w_2 . The relationships between maximum absolute gain and w_2 and between radiation efficiency and w_2 are shown in **Fig. 4**. Here, the substrate thickness parameters were the same. In this figure, it is clear that the maximum absolute gain is 11.1 dBi and that the radiation efficiency is 91% when w_1 is $0.22 \lambda_0$ and w_2 is $0.28 \lambda_0$. The antenna achieves the maximum radiation efficiency of 97% when w_2 is $0.32 \lambda_0$. We

believe that, in this case, the peak of the absolute gain is obtained by increasing the antenna aperture as the number of parasitic elements increases and the efficiency degrades due to the decrease in the coupling between the feed element and the parasitic elements. Additionally, it is necessary to clarify the effect of substrate thickness on the parasitic elements. The dependence of the absolute gain on the substrate thicknesses, t_1 and t_2 , is shown in **Fig. 5**. When t_1 and t_2 are 0.25 and 0.55 mm, respectively, the absolute gain has the maximum value of 11.1 dBi. Additionally, it is clear that the manufacturing margins of t_1 and t_2 are approximately 150 and 100 μm , respectively, and the gain reduction is less than 0.5 dB. Furthermore, it is clear that the precision of the substrate thickness of the conventional multilayer Teflon substrate process is sufficient to construct this proposed antenna. The antenna's frequency characteristics (**Fig. 6**) show that the bandwidth is 2.6% when the S_{11}

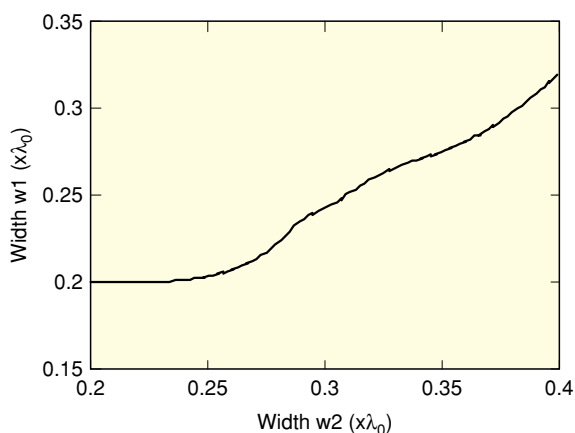


Fig. 3. Relationship between w_1 and w_2 that achieves the maximum absolute gain.

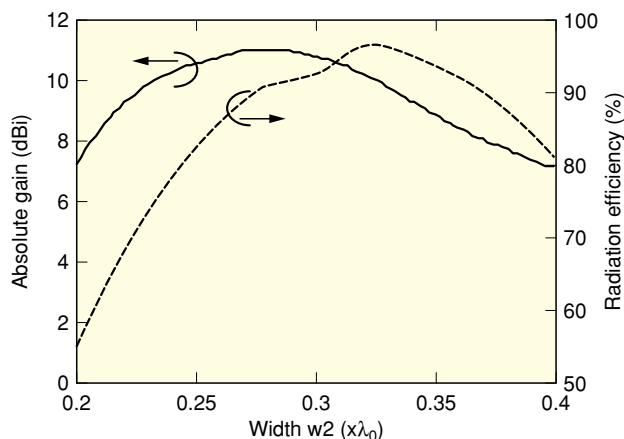


Fig. 4. Absolute gain and radiation efficiency characteristics versus w_2 .

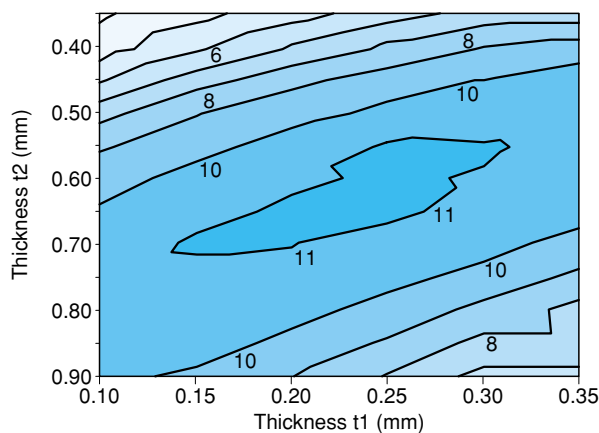


Fig. 5. Absolute gain characteristics versus substrate thicknesses t_1 and t_2 .

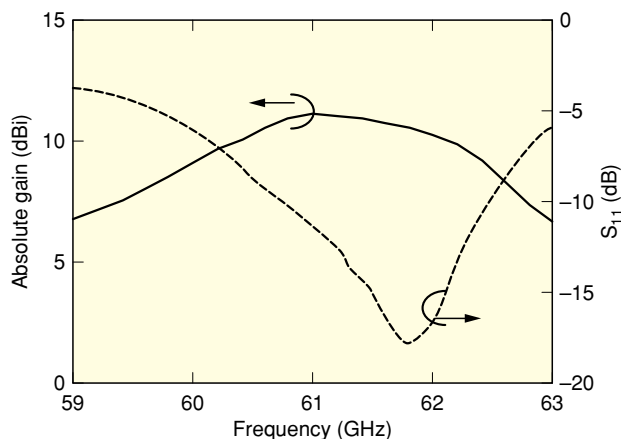
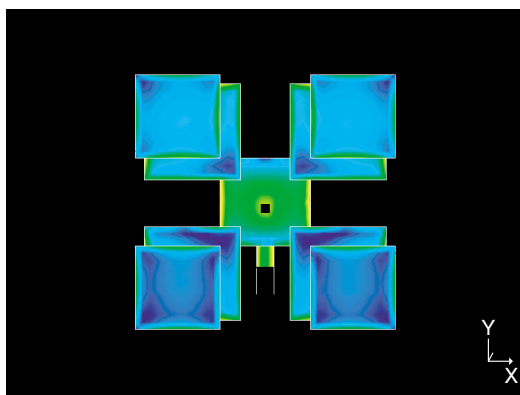


Fig. 6. Calculated frequency characteristics of the absolute gain and S_{11} .

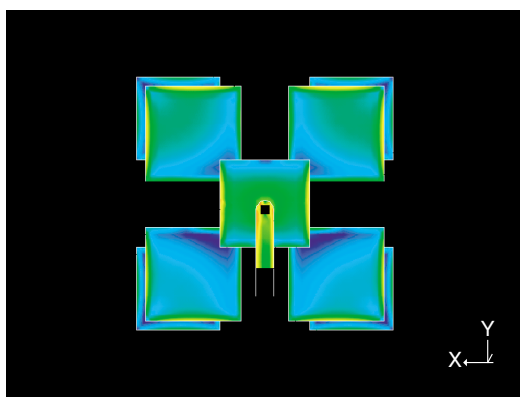
characteristics are less than -10 dB. To consider the mechanism of this antenna, we calculated the current distribution using the moment method analysis. The results in Fig. 7 show that in the feeding element, the current is distributed to the first layer parasitic elements and via them to the second-layer parasitic elements. The RF signal can be effectively separated from the feeding element and passed to the second-layer parasitic elements without using a power divider circuit, so array operation can be achieved.

2.3 Effect of the substrate on MPMAA

To make the system-on-package module, we investigated several substrates. In this section, we describe the dependence of the antenna's performance on the key substrate characteristic: the effective dielectric constant. Figure 8 shows the positions of the parasitic elements that give maximum antenna gain as a function of the effective dielectric constant of a sub-



(a) Front view



(b) Rear view

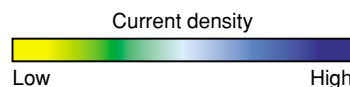


Fig. 7. Current distribution of the proposed antenna.

strate. The corresponding maximum antenna gain is plotted in Fig. 9. As the effective dielectric constant of the substrate increased, w_1 and w_2 decreased. They saturated when the effective dielectric constant was more than 7.5. On the other hand, the corresponding maximum gain continuously decreased. However, the MPMAA fabricated on an LTCC substrate ($\epsilon_r = 7.7$, $\tan\delta = 0.002$ at 10 GHz) achieved antenna gain of more than 8 dBi. These results indicate that our MPMAA can offer reasonable antenna gain even if we use low-cost materials, such as LTCC or high-temperature cofired ceramic (HTCC), for the substrate.

3. Effect of alignment precision

The antenna constructed on a multilayered Teflon substrate that binds the substrates using a bonding

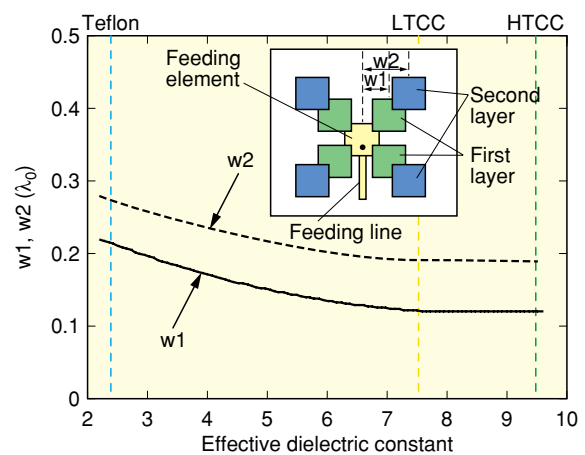


Fig. 8. Positions of parasitic elements for maximum antenna gain versus effective dielectric constant.

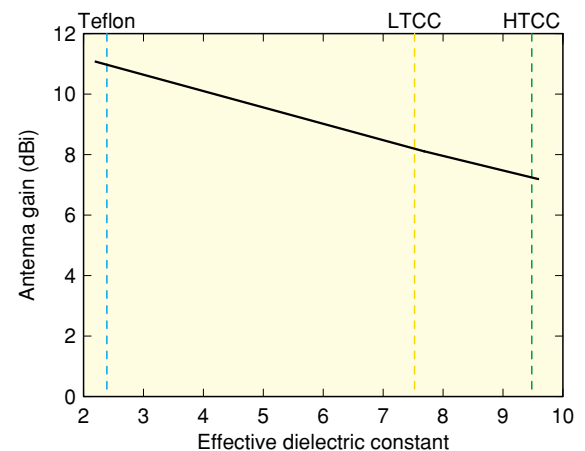


Fig. 9. Antenna gain versus effective dielectric constant.

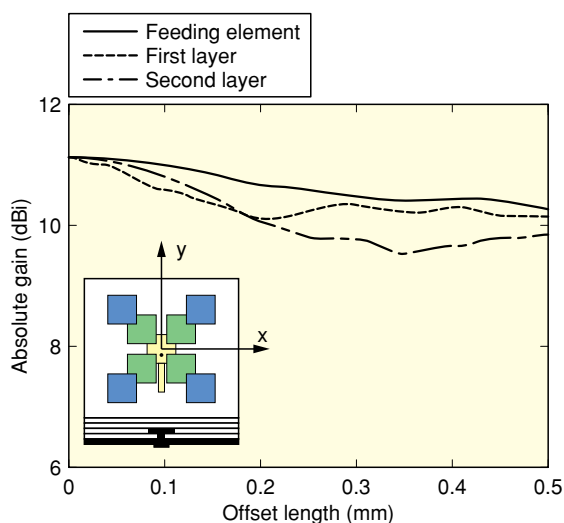


Fig. 10. Absolute gain reduction versus alignment precision of x-axis direction.

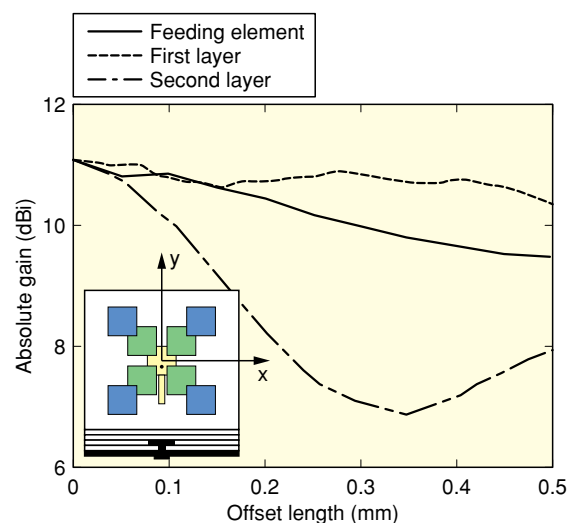


Fig. 11. Absolute gain reduction versus alignment precision of y-axis direction.

film is more sensitive to alignment precision than antennas on other substrates such as an alumina-ceramic substrate. Therefore, we need to clarify the effect of alignment error due to the binding substrates. We used the moment method for the calculation. The size of the feeding element was $0.30 \lambda_0 \times 0.30 \lambda_0$ and the feeding point was $0.01 \lambda_0$ away from the center of the patch. The size of the parasitic elements mounted on the first parasitic layer was $0.32 \lambda_0 \times 0.32 \lambda_0$ and the patch size of the second parasitic layer was $0.28 \lambda_0 \times 0.28 \lambda_0$. Furthermore, the position of the first parasitic layer was $x: \pm 0.22 \lambda_0, y: \pm 0.22 \lambda_0$ and the position of the second parasitic layer was $x: \pm 0.28 \lambda_0, y: \pm 0.28 \lambda_0$. The calculated absolute gain reductions when alignment errors occur in the direction of the x- and y-axes are shown in **Figs. 10** and **11**, respectively. Alignment errors in the y-axis direction clearly had a greater effect than those in the x-axis direction. We believe this is because there was a standing wave in the direction of the y-axis of each patch. Moreover, it is clear that the alignment margins of the first-and second-layer parasitic substrate are approximately ± 100 and ± 50 μm , respectively, and that the gain reduction is less than 0.5 dB. Furthermore, the simulation results indicate that the alignment precision of the conventional multilayer Teflon substrate process is sufficient to construct this antenna.

4. Measured performance

4.1 Measurement system

In the millimeter-wave frequency range, one impor-

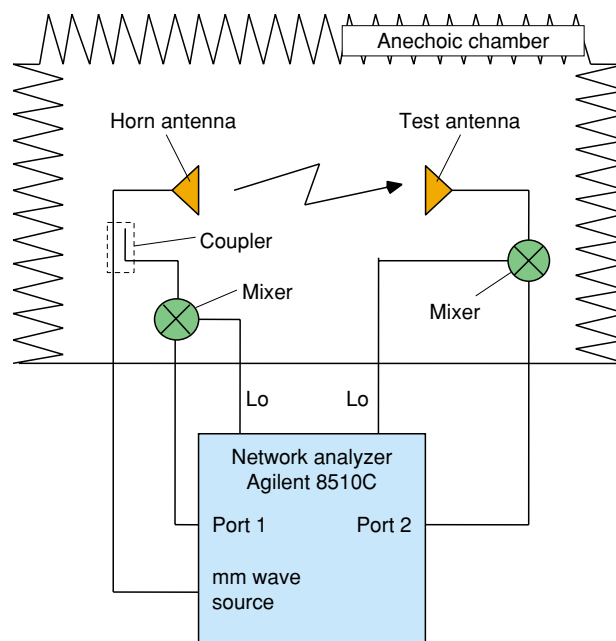


Fig. 12. Antenna pattern measuring system.

tant issue is the effect on measured values of soldering errors and differences in the connecting torque. To eliminate this deviation, we developed a novel antenna-probing fixture based on an RF on-wafer probing system. As a result, we obtained the same measurement accuracy as for MMIC chip measurements for the radiation pattern of miniaturized antennas in the millimeter-wave frequency band. Our millimeter-wave radiation pattern measuring system is shown in **Fig. 12**. The configuration using an RF

probe is shown in **Fig. 13** and a photograph of the system is shown in **Fig. 14**. These on-wafer probes can be directly connected to an antenna terminal formed on the planar substrate. This system can measure the antenna radiation without the need to mount RF connectors on the antenna substrate. This method yields higher accuracy and higher efficiency. This fixture has two probe heads. One probe is used to feed the RF signal to the antenna terminal and the other is used to feed the control signal and DC power to the devices mounted on the antenna substrate.

4.2 MPMAA on Teflon substrate

We manufactured a prototype antenna with a Teflon substrate to confirm the design for the 60-GHz band. We used a microstrip line (MSL) and a via hole to feed the MSA, which acted as the feeding element shown in Fig. 2. Two parasitic layers were arranged so that the size and location of the MSA and parasitic elements, the substrate thickness, and the location of the feeding points yielded the maximum absolute gain as described in the previous section. A photograph of the prototype antenna is shown in **Fig. 15**. The left side shows a side view of the antenna element and the right side shows the feeding line. The fabricated prototype antenna chip size is 10.0 mm × 10.0 mm × 1.1 mm. The E-plane and H-plane radiation patterns are shown in **Fig. 16**. The measured and calculated radiation patterns had fairly similar main lobes.

Next, we discuss the bandwidth of this antenna. The frequency characteristics of the measured maximum gain and the S_{11} characteristics are shown in **Fig. 17**. The frequency bandwidth for the gain that is 3 dB below the peak gain for this antenna is from 59.3 to 62.6 GHz. Therefore, the bandwidth compared with the center frequency is 5.5%. The S_{11} frequency characteristics and the gain are in good agreement with the calculated results shown in Fig. 6. Moreover, we can see that the estimated absolute gain is greater than 8.5 dBi because the measured absolute gain of this antenna is greater than 7.4 dBi including the RF probe loss, which is approximately 1.1 dB at 60 GHz. The difference between the calculated and measured gains is approximately 3 dB. Here, we discuss three possible causes for this gain reduction: 1) loss in the microstrip line or coplanar line transition, 2) a discrepancy between the designed and actual values of the bonding film thickness resulting from the manufacturing process, and 3) the fabrication accuracy in the antenna manufacturing process. More specifically, the gain reduction due to the change in bonding

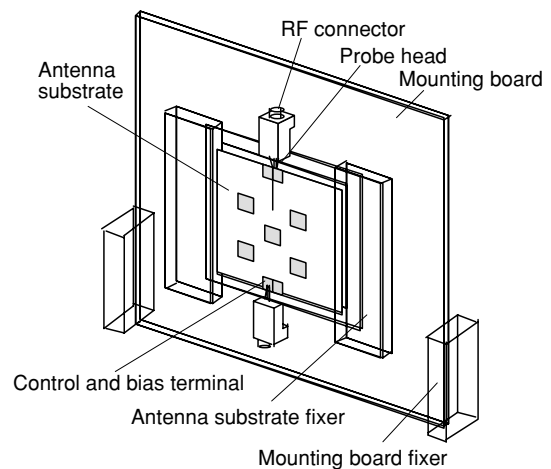


Fig. 13. Configuration of measuring system using an RF probe.

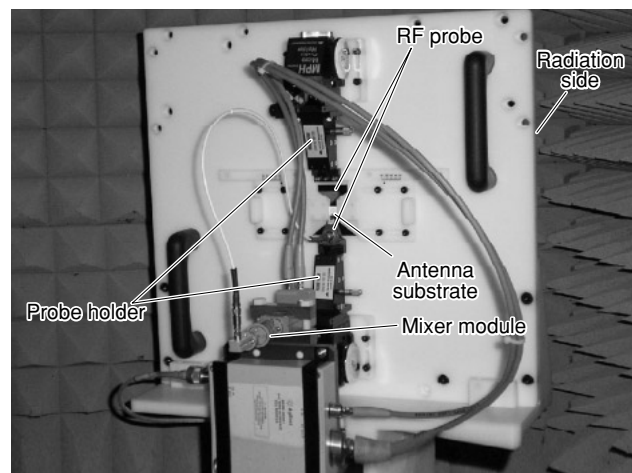


Fig. 14. Photograph of measuring system using an RF probe.

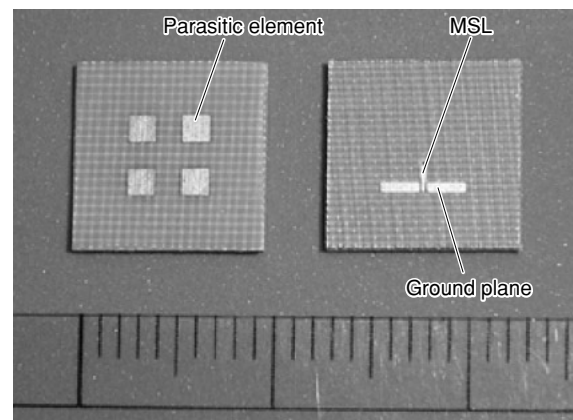


Fig. 15. Photograph of MPMAA fabricated on Teflon substrate.

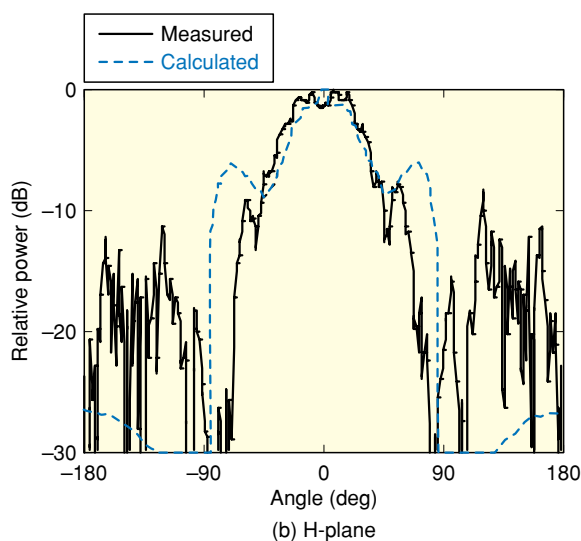
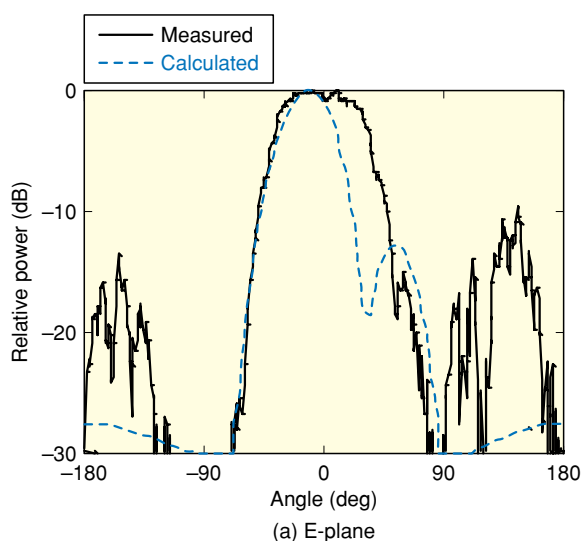


Fig. 16. Measured radiation pattern of MPMAA on Teflon substrate.

film thickness was at least 1 dB, even when the antenna's alignment accuracy at the time of manufacture was approximately 100 μm . One topic for future study is to find a bonding film material that has electrical characteristics similar to the Teflon substrate. Furthermore, it seems that the alignment binding accuracy of the multilayer Teflon substrate needs to be improved to approximately 50 μm .

4.3 MPMAA on LTCC substrate

A photograph of the prototype antenna fabricated on an LTCC substrate is shown in Fig. 18. The left side shows a side view of the antenna element and the right side shows the feeding line. The radiation characteristics of the prototype antenna are shown in Fig.

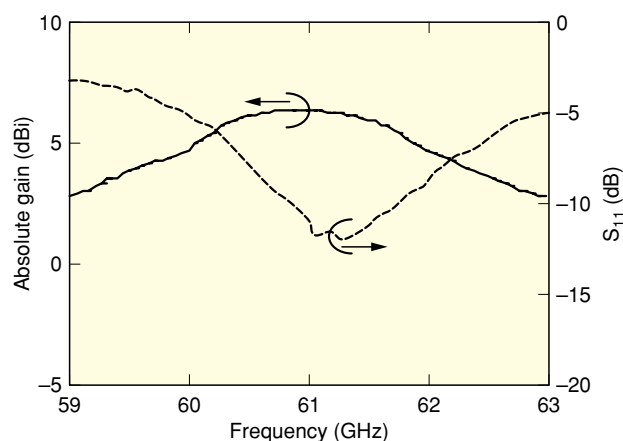


Fig. 17. Absolute gain and S_{11} of MPMAA on Teflon substrate.

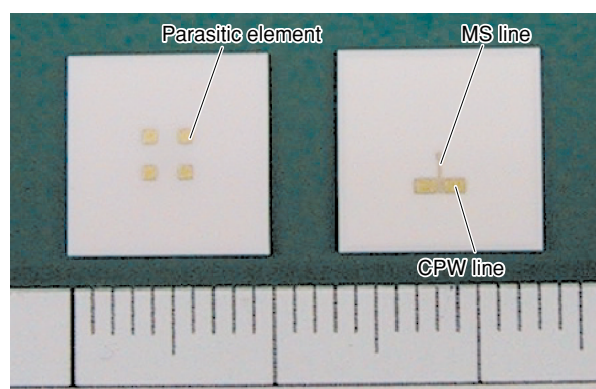


Fig. 18. Photograph of MPMAA fabricated on LTCC substrate.

19. The measured and calculated main lobe characteristics are in good agreement. Furthermore, we clarified that the measured absolute gain of this antenna is 7.17 dBi including the RF probe loss, which is approximately 1.2 dB at 60 GHz. The frequency bandwidth for the gain that is 3 dB below the peak gain for this antenna is from 59.3 to 61.3 GHz. Therefore, the bandwidth compared with the center frequency is 3.3%.

5. Conclusion

We described a highly efficient multilayer parasitic microstrip antenna array (MPMAA) constructed on a multilayer substrate for millimeter-wave system-on-package modules. The basic design and performance of the array antenna were described when a Teflon substrate was used. We also described the effects of the substrate and the alignment of parasitic elements

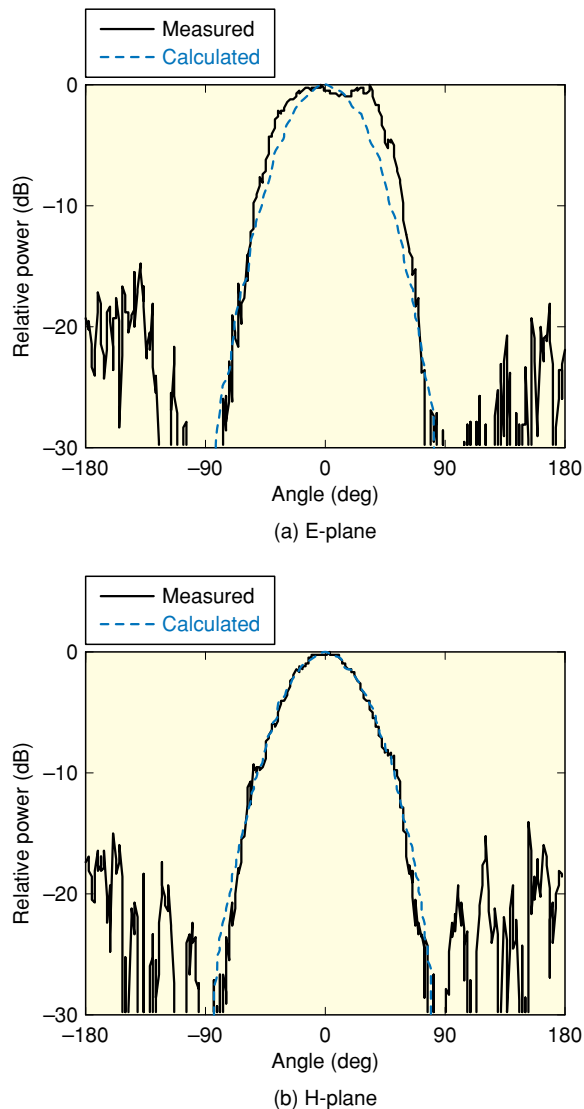


Fig. 19. Measured radiation pattern of MPMAA on LTCC substrate.

on antenna performance. The radiation efficiency and associated antenna gain of the antenna on a Teflon substrate were greater than 91% and 11.1 dBi, respectively. We discussed fabricated 60-GHz-band MPMAAs on both Teflon and LTCC substrates and presented performance measurement results. The MPMAA offers compactness and high efficiency and is suitable for system-on-package modules. Thus, it enables us to make compact and cost-effective millimeter-wave RF modules.

References

- [1] Y. Takimoto, "Recent activities on millimeter wave indoor LAN system development in Japan," in 1995 IEEE MTT-S Int. Microwave Symp. Dig., pp. 405-408, June 1995.
- [2] N. Morinaga and A. Hashimoto, "Technical trend of multimedia mobile and broadband wireless access systems," IEICE Trans. B, Vol. E82-B, No. 12, pp. 1897-1905, Dec. 1999.
- [3] T. Ihara and K. Fujimura, "Research and development of millimeter-wave short-range application systems," IEICE Trans. B, Vol. E79-B, No. 12, pp. 1741-1753, Dec. 1996.
- [4] T. Nakagawa, K. Nishikawa, B. Piernas, T. Seki, and K. Araki, "60-GHz antenna and 5-GHz demodulator MMICs for more than 1-Gbps FSK transceivers," in Proc. 32nd European Microwave Conf., pp. 929-932, Sep. 2002.
- [5] Y. Hirachi, H. Nakano, and A. Kato, "A cost-effective RF-module with built-in patch antenna for millimeter-wave wireless systems," in Proc. 29th European Microwave Conf., pp. 347-350, Oct. 1999.
- [6] M. Tentzeris, N. Bushyager, J. Laskar, G. Zheng, and J. Papapolymerou, "Analysis and design of MEMS and embedded components in Silicon/LTCC packages using FDTD/MRTD for system-on-package (SOP)," in Proc. Silicon Monolithic Integrated Circuits in RF Systems, 2003 Topical Meeting, pp. 138-141, Apr. 2003.
- [7] U. Sangawa, T. Urabe, Y. Kudoh, A. Omote, and K. Takahashi, "A study on a 60 GHz low profile dielectric lens antenna using high-permittivity ceramics -toward a low profile antenna," Technical report of IEICE, MW2002-116, pp. 57-62, Nov. 2002.
- [8] J. Lin and T. Itoh, "Active integrated antennas," IEEE Trans. Microwave Theory and Tech., Vol. 42, pp. 2186-2194, Dec. 1994.
- [9] T. Seki, H. Yamamoto, T. Hori, and M. Nakatsugawa, "Active antenna using multilayer ceramic-polyimide substrates for wireless communication systems," in 2001 IEEE MTT-S Int. Microwave Symp. Dig., pp. 385-388, May 2001.
- [10] T. Seki, K. Cho, and H. Mizuno, "Novel active integrated antenna configuration using multilayer Teflon substrate and solder bump interconnection," in Proc. 32nd European Microwave Conf., pp. 605-608, Sep. 2002.
- [11] H. Legay and L. Shafai, "A new stacked microstrip antenna with large bandwidth and high gain," in Proc. 1993 IEEE AP-S Int. Symp., pp. 948-951, July 1993.
- [12] S. D. Targonski, R. B. Waterhouse, and D. M. Pozar, "Design of wide-band aperture-stacked patch microstrip antennas," IEEE Transactions on Antennas and Propagation, Vol. 46, pp. 1245-1251, Sep. 1998.
- [13] R. B. Waterhouse, "Stacked patches using high and low dielectric constant material combinations," IEEE Transactions on Antennas and Propagation, Vol. 47, pp. 1767-1771, Dec. 1999.
- [14] R. Li, G. Dejean, M. Maeng, K. Lim, S. Pinel, M. M. Tentzeris, and J. Laskar, "Design of compact stacked-patch antennas in LTCC multilayer packaging modules for wireless applications," IEEE Transactions on Advanced Packaging, Vol. 27, No. 4, pp. 581-589, Nov. 2004.
- [15] E. Nishiyama, M. Aikawa, and S. Egashira, "Three-Element stacked microstrip antenna with wide-band and high-gain performances," 2003 Int. IEEE AP-S Symp. Dig., Vol. 2, pp. 900-903, June 2003.
- [16] T. Seki, K. Nishikawa, and K. Cho, "Multilayer parasitic microstrip array antenna on LTCC substrate for millimeter-wave system-on-package," in Proc. 33rd European Microwave Conf., pp. 1393-1396, Oct. 2003.
- [17] T. Seki, N. Honma, K. Nishikawa, and K. Tsunekawa, "High efficiency multilayer parasitic microstrip array antenna on Teflon substrate," in Proc. 34th European Microwave Conf., pp. 829-832, Oct. 2004.



Tomohiro Seki

Research Engineer, Wireless Systems Innovation Laboratory, NTT Network Innovation Laboratories.

He received the B.E. and M.E. degrees in electrical engineering from Tokyo University of Science, Tokyo in 1991 and 1993, respectively. In 1993, he joined NTT Radio Communication Systems Laboratories (now NTT Network Innovation Laboratories), Kanagawa. He has been engaged in the development of array antennas and active antennas for the millimeter-wave and microwave bands. He received the Young Engineer Award from the Institute of Electronics, Information and Communication Engineers (IEICE) in 1999. He is a member of IEEE and IEICE.



Kenjiro Nishikawa

Senior Research Engineer, Wireless System Innovation Laboratory, NTT Network Innovation Laboratories.

He received the B.E. and M.E. degrees in welding engineering and Dr. Eng. degree in communication engineering from Osaka University, Suita, Osaka in 1989, 1991, and 2004, respectively. In 1991, he joined NTT Radio Communication Systems Laboratories (now NTT Network Innovation Laboratories), Kanagawa, where he has been engaged in R&D of three-dimensional and uniplanar monolithic MMICs on Si and GaAs and their applications. He is currently interested in millimeter-wave transceivers, system-on-package technologies, active integrated antennas, and high-speed communication systems. He is a Technical Program Committee member of the IEEE Compound Semiconductor Integrated Circuit Symposium and the IEEE Radio and Wireless Symposium. He is a member of IEEE and IEICE of Japan. He received the 1996 Young Engineer Award from IEICE.



Ichihiko Toyoda

Senior Research Engineer, Wireless Systems Innovation Laboratory, NTT Network Innovation Laboratories.

He received the B.E., M.E., and Dr. Eng. degrees in communication engineering from Osaka University, Suita, Osaka in 1985, 1987, and 1990, respectively. In 1990, he joined NTT Radio Communication Systems Laboratories, Kanagawa, where he was engaged in developmental research based on electromagnetic analysis for three-dimensional and uniplanar MMICs. From 1994 to 1996, he was with NTT Electronics Technology Corporation, Kanagawa, where he was engaged in the development of wireless communication equipment and MMICs. From 1996 to 1997, he was with NTT Wireless Systems Laboratories, Kanagawa, where he performed R&D of highly integrated multifunctional MMICs, high-frequency Si MMICs, and MMIC design software based on 3-D masterslice MMIC technology. From 1997 to 2001, he was engaged in the development of ultrahigh-speed digital ICs and MMICs for optical and wireless communication systems as Engineering Director of IC Design at NTT Electronics Corporation, Kanagawa. His current interests concern millimeter-wave and quasi-millimeter-wave high-speed wireless access systems and their applications. Since 2004, he has also been a Visiting Associate Professor at Niigata University. He received the 1993 IEICE Young Engineer Award, the Japan Microwave Prize presented at the 1994 Asia-Pacific Microwave Conference in Tokyo, the 18th Telecom System Technology Award from the Telecommunications Advancement Foundation, and the 2005 IEICE Electronics Society Award. He is a member of IEICE and IEEE.



Koichi Tsunekawa

Senior Manager, Executive Research Engineer, Wireless Systems Innovation Laboratory, NTT Network Innovation Laboratories.

He received the B.S., M.S., and Ph.D. degrees in engineering science from the University of Tsukuba, Tsukuba, Ibaraki in 1981, 1983, and 1992, respectively. He joined the Electrical Communications Laboratories of Nippon Telegraph and Telephone Public Corporation (now NTT), Tokyo in 1983. Since 1984, he has been engaged in R&D of portable telephone antennas in land mobile communication systems. From 1993 to 2003, he was with NTT DoCoMo, Inc. where he worked on radio propagation research, intelligent antenna systems for wireless communications, and the development of IMT-2000 antenna systems. His research interests are antenna systems for MIMO transmission, millimeter-wave broadband access, and ubiquitous wireless systems. He is a member of IEICE and IEEE.